Quasiperiodically driven maps in the low-dissipation limit

Shakir Bilal[1] and Ramakrishna Ramaswamy[1,2]
[1]*School of Physical Sciences, Jawaharlal Nehru University, New Delhi 110 067, India*
[2]*University of Hyderabad, Hyderabad 500 046, India*

(Received 24 September 2012; revised manuscript received 18 February 2013; published 11 March 2013)

We study the quasiperiodically driven Hénon and Standard maps in the weak dissipative limit. In the absence of forcing, there are a large number of coexisting periodic attractors. Although chaotic attractors can also be found, these typically have vanishingly small basins of attraction. Quasiperiodic forcing reduces the multistability in the system, and as the bifurcation parameter is varied, strange nonchaotic attractors (SNAs) are created. The attractor basin for SNAs appears to be the largest among those of all coexisting attractors at such a transition.

DOI: 10.1103/PhysRevE.87.034901 PACS number(s): 05.45.Ac, 05.45.Gg

I. INTRODUCTION

Both the nature of the dynamics as well as the bifurcations in simple dynamical systems are significantly modified in the presence of external forcing [1–3]. Depending on whether the unforced system is conservative or dissipative, different behaviors can result [4–6], and these issues have been studied extensively over the years with particular focus on the different dynamical attractors that can be formed, the various transitions that take place, and their potential applications [3,4]. Additionally, different types of forcing—most notably random and quasiperiodic modulation—have been studied extensively. Noise has been shown to be effective in controlling the dynamics in multistable systems [1,2,7,8] or in enabling escape [9]. Quasiperiodic forcing of dissipative systems also results in stabilization, but through the creation of strange nonchaotic attractors (SNAs), namely dynamics with no positive Lyapunov exponents and with an underlying fractal geometry [4].

How do the attractors in forced and damped systems evolve as the damping is turned off? The conservative limits of many dynamical systems have been studied in detail [6,10,11]; when this limit is Hamiltonian, the dynamics is either on n-dimensional tori in the phase space, or in the chaotic web [12]. Externally forced weakly dissipative systems have been studied earlier [4] for the case of noisy forcing [1,2,7]. A parallel investigation of the dynamics with quasiperiodic modulations thus seems appropriate. Furthermore, the Hénon map with high dissipation has also been studied with quasiperiodic forcing [13].

In the absence of forcing, it is known that for large dissipation, typically a single attractor is observed for a given value of the nonlinearity parameter. As the conservative limit is approached, however, multistability is abundant: most of the attractors are periodic orbits, and chaotic attractors are relatively rare [14]. Further, these also tend to have exponentially small basins of attraction and are difficult to detect. With quasiperiodic forcing we find that multistability persists depending on forcing strength, but the SNAs have a large basin of attraction.

This paper is organized as follows. In the following section, we recall the properties of the weakly dissipative regime that are germane to the present study. In Sec. III we consider the dynamics of the Hénon and Standard mappings with a quasiperiodic drive. This is followed in Sec. IV by a discussion and summary of our results.

II. THE WEAK DISSIPATION LIMIT

For nearly conservative dynamical systems, we confine our attention here to the following situation. Consider a conservative system for which the motion is on quasiperiodic tori, or is chaotic [12]. If a sufficiently small dissipative term is added to the dynamical equations, the resulting dissipative system possesses invariant sets; this is analogous to the Kolmogorov-Arnold-Moser (KAM) theorem that holds in conservative Hamiltonian systems [5]. Each initial condition in a conservative system leads to a different marginally stable orbit, namely a periodic orbit or a chaotic island [12]. With weak dissipation, some of the invariant structures that are present in the conservative limit become attractors or semiattractors [15].

The large number of periodic orbits in a conservative system evolve into a large but finite number of periodic attractors with the introduction of weak dissipation. The number of attractors depends on the family of mappings considered as well as the amount of dissipation introduced [16]. The chaotic sea in the conservative case evolves into the complex basin boundaries of the coexisting periodic attractors. Both the area occupied by the chaotic attractors in parameter space as well as their basin sizes reduce upon reducing the dissipation. These features of the transition from dissipative to conservative systems have been studied numerically in a number of such systems [16,17], most notably the Hénon and Standard maps. These are respectively defined by the equations

$$x_{n+1} = 1 - ax_n^2 - (1-\nu)y_n, \quad y_{n+1} = x_n \tag{1}$$

for the Hénon mapping [16,18], and

$$\begin{aligned} x_{n+1} &= (1-\nu)x_n + a\sin(x_n + y_n), \\ y_{n+1} &= y_n + x_n \mod 2\pi \end{aligned} \tag{2}$$

for the Standard mapping [19], where $2 \leqslant \nu \leqslant 0$ and a are the dissipation and nonlinearity parameters respectively, with $\nu = 0,2$ being the conservative cases.

III. QUASIPERIODIC DRIVING

We now introduce an external quasiperiodic drive,

$$\begin{aligned} x_{n+1} &= G(x_n, y_n, \alpha) + \epsilon\cos 2\pi\theta_n. \\ \theta_{n+1} &= \theta_n + \omega \bmod 1, \end{aligned} \tag{3}$$

 ©2013 American Physical Society

$G(x_n, y_n, \alpha)$ being the unforced Hénon or Standard map. The θ dynamics is an irrational rotation, with $2\omega = \sqrt{5} - 1$. Earlier studies of strongly dissipative discrete maps with quasiperiodic forcing [13] reported the creation of SNAs via the collision route, when a period-doubled torus occupies the same region of phase space as its unstable parent [20], as well as fractalization [21]. We restrict ourselves to cases in which ν is close to 0 or 2, and we study the evolution of the basin of SNAs. A number of order parameters have been devised to detect and characterize SNAs. By taking successive rational approximations to the forcing frequency ω (here the inverse golden mean ratio), namely $\omega_k = F_{k-1}/F_k$, where F_k are the Fibonacci numbers, one can systematically investigate the dynamics. The initial driving angle θ_0 in the range $0 \leqslant \theta_0 < 1/F_k$ is taken as a parameter to obtain a bifurcation diagram that can reveal the chaotic regions that contribute to the strange dynamics [4]. The distribution of finite-time Lyapunov exponents (FTLEs) $P(\lambda, N)$ also reveals the finite length chaotic sets embedded in a trajectory. The fraction of positive FTLEs, F_+, as a function of subtrajectory length N,

$$F_+(N) = \int_0^\infty P(\lambda, N) d\lambda, \tag{4}$$

is known to decrease with increasing subtrajectory length N and shows a scaling behavior in the large-N limit for intermittent SNAs and exponential for the SNAs created via fractalization [22].

Another useful quantity that correlates with the fractal geometry of SNAs is the phase-sensitivity exponent $\Gamma(N)$, namely the slope of the envelope of the following quantity [4]:

$$\gamma(N) = \max_{0 \leqslant k \leqslant N} \left(\left| \frac{\partial x_k^1}{\partial \theta} \right| \right); \tag{5}$$

a power-law growth of $\Gamma(N)$ is indicative of an SNA.

The evolution of the basin of attraction of SNAs can be studied via the mean-square displacement $\langle r^2 \rangle$ [23] as its signature in the phase space. If ψ is any of the phase-space coordinates and ψ_{ref} is taken as a reference point (here we use $\psi_{\text{ref}} = 0.001$), then

$$\langle r^2 \rangle = \frac{1}{M} \sum_{i=1}^{M} (\psi - \psi_{\text{ref}})^2 \tag{6}$$

clusters around a single value for each coexisting attractor. Furthermore, this quantity converges rapidly with M and thus provides a good measure in counting the number of coexisting attractors in addition to providing an estimation of basin sizes.

A. The driven Hénon map

Substituting the Hénon map for $G(x_n, y_n, \alpha)$ in Eq. (3), we find that with decreasing dissipation the regions of *bounded* dynamics are severely reduced in the parameter space comprising a, ν, and ϵ. Here we restrict attention to the a-ν plane in order to make comparisons with analogous results in the unforced case. The dynamical regimes with a particular choice of ϵ are shown in Fig. 1 (cf. Fig. 5 in Ref. [16]). For a fixed parameter set indeed most orbits escape, and for those that do not, one such representative case at the interface of chaotic and quasiperiodic dynamics is shown in Fig. 2. We

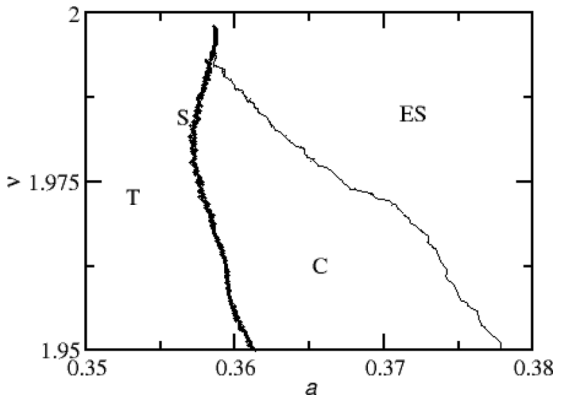

FIG. 1. Schematic diagram showing different dynamical regimes in the a-ν plane for the Hénon map with $\epsilon = 0.26$. The regions corresponding to chaotic motion are marked C, torus dynamics are T, escape regions are ES, and S is the line along which SNAs occur, and these have been investigated here.

next analyze the basins of typical SNAs. We locate SNAs in the phase space (along with other coexisting attractors) with mean-square displacement $\langle r^2 \rangle$, Eq. (6). After removing $\sim 10^6$ transients, we iterate 10^6 initial conditions chosen in the box, $[x, y] = [-4, 4] \times [-4, 11]$, since it contains all the bound orbits of the unforced case. We keep the initial phase $\theta_0 = 0$ (other choices do not alter the basic results). We find that the bound dynamics in the chosen phase-space region corresponds to SNAs, although other attractors may coexist. Multistability is reduced depending on forcing strength, and this makes attractors with small basins difficult to locate. A typical SNA and its basin are shown in Fig. 2 and the corresponding histogram of $\langle r^2 \rangle$ is shown in Fig. 3. Each peak in the histogram represents a possible distinct attractor. Despite there being multiple blocks in the histogram of comparable height, the basin for each of these blocks is found to indicate the same SNA: if the basins are intertwined, numerical uncertainty makes it very difficult to find the other attractors. We analyzed

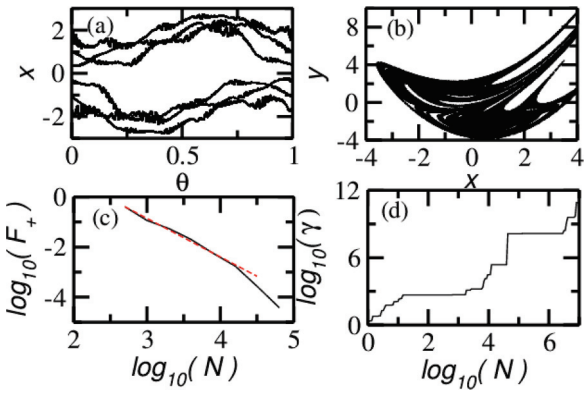

FIG. 2. (Color online) (a) A typical SNA along the line "S" in Fig. 2. (b) Basin of the SNA as obtained via computation of $\langle r^2 \rangle$. (c) The area under the finite-time largest Lyapunov exponent distribution corresponding to positive values F_+ (black) as a function of trajectory length N for the SNA in (a). The linear region (dashed red) has a slope ~ -1.54. (d) Phase sensitivity parameter for the SNA. The system parameter values are $a = 0.356\,85$, $\nu = 1.98$, and $\epsilon = 0.26$.

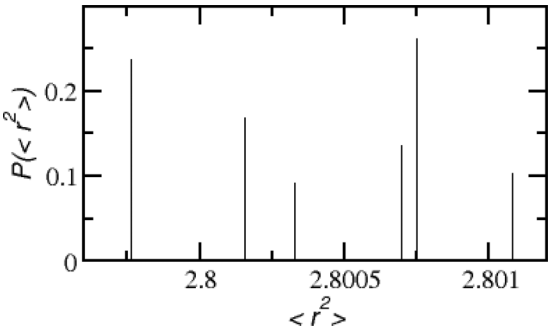

FIG. 3. Histogram of mean-square displacements $\langle r^2 \rangle$ of the y coordinate for the attractors formed in the basin shown in Fig. 2(b) for the Hénon map. Notice the $\langle r^2 \rangle$ has a small extent, indicating a single attractor. The system parameter values are $a = 0.356\,85$, $\nu = 1.98$, and $\epsilon = 0.26$.

SNAs at low-dissipation values using the phase-sensitivity parameter γ, rational approximations, and the fraction of positive FTLE's, $F_+(N)$. Each of these measures confirms that SNAs do exist for lower and lower dissipation, but obtaining rational approximations to the attractors presents difficulties if appropriate initial conditions are not chosen for a given ω_k due to the fractal nature of the basins in the x_0-y_0-θ_0 space. We choose appropriate initial condition from the slice $y_0 = 1.5$ and obtain the rational approximation to the SNA; see Fig. 4.

Quasiperiodic forcing of the system thus gives SNAs at the interface of quasiperiodic tori and chaotic dynamics in a-ν-ϵ space. We have analyzed them in the low-dissipation regime for fixed ϵ, and when there is multistability, SNA basins are the largest among all coexisting attractors.

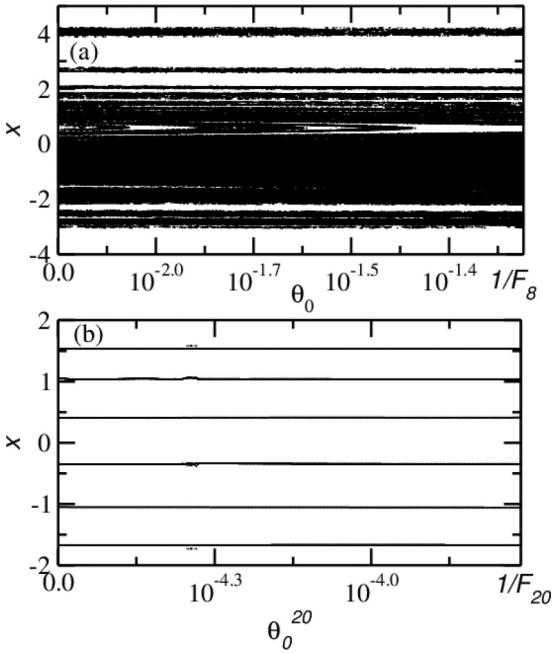

FIG. 4. (a) Basin of the eighth rational approximation to an SNA in the Hénon map at $a = 0.356\,85$, $\nu = 1.98$, and $\epsilon = 0.26$ in the θ_0-x plane. Here $y_0 = 1.5$ is held fixed. Notice that the θ axis is shown up to $1/F_8$. (b) 20th rational approximation of the SNA; notice the small bifurcation features indicating that the attractor is indeed fractal.

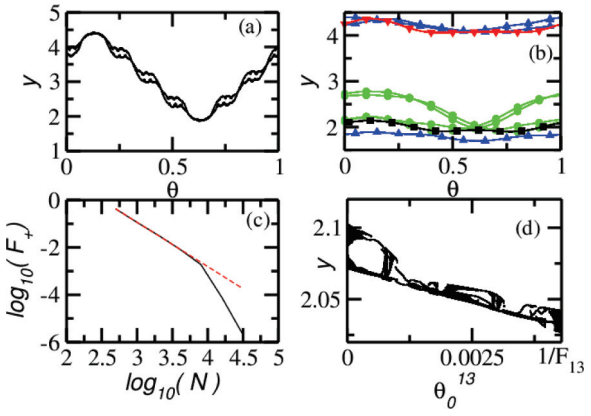

FIG. 5. (Color online) (a) An SNA observed in the Standard map for parameters $\nu = 0.02$, $a = 3.8774$, and $\epsilon = 0.2$; (b) some of the other coexisting orbits for the same parameter values (circle, square, triangle-up, triangle-down); (c) the quantity F_+ (black) for the SNA in (a) and its linear fit (dashed red) with slope ~ -1.87; and (d) its rational approximation with $\omega_{13} = 144/233$.

B. The driven Standard map

In the quasiperiodically driven Standard map as well, there is typically a single SNA at the interface of chaos and regular dynamics for large dissipation. With forcing, the multistability that can be observed in the unforced map [19] is reduced (see Figs. 5 and 6) to an extent that depends on forcing strength. For instance, there are five coexisting orbits for the parameter set $a = 3.8774$, $\nu = 0.02$, and $\epsilon = 0.2$, with one of them being an SNA as can be seen in Fig. 5. In comparison, in the unforced case as discussed by Feudel *et al.* [19], more than 200 coexisting attractors can be found.

The quantity F_+ and the rational approximation for the SNA are shown in Figs. 5(c) and 5(d). Basin analysis reveals that the SNA occupies a significant fraction of the phase space, Figs. 6 and 7. Using the Lyapunov exponent as an indicator for the transition from regular to chaotic dynamics, the search for SNAs has to be performed in a narrow range of the parameter a. This is difficult to locate to great precision, and long chaotic transients make the detection of SNAs even more difficult. For dissipation as low as $\nu = 0.01$, even after removing transients of length 5×10^9, the nonchaotic nature of the attractor was difficult to discern.

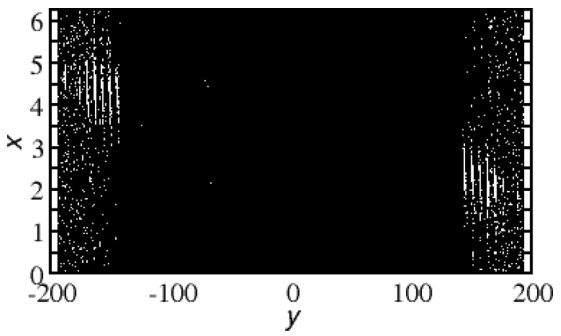

FIG. 6. Basin of attraction for the SNA in Fig. 5(a) (black) and other coexisting orbits (white) in the Standard map. The parameters are $\nu = 0.02$, $a = 3.8774$, and $\epsilon = 0.2$.

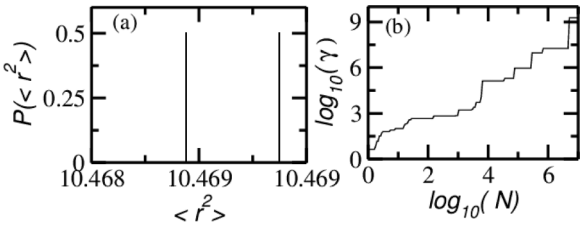

FIG. 7. (a) Histogram of mean-square displacements $\langle r^2 \rangle$ in the basin of SNA, black region in Fig. 6, and (b) phase-sensitivity parameter γ for the SNA.

IV. DISCUSSION AND SUMMARY

In this paper, we have studied the quasiperiodically driven Standard and Hénon mappings in the low-dissipation regime. In the conservative limit, there can be no attractors and thus no possibility of strange nonchaotic dynamics, but for weak dissipation, SNAs can be found. The addition of quasiperiodic driving converts the numerous periodic attractors in weakly dissipative systems into a relatively small number of attractors, and when there is an SNA, we find that it has the largest basin among all coexisting attractors.

In contrast, when there is no forcing, chaotic attractors are rare in the weakly dissipative limit in these maps (the behavior is generic as argued in Ref. [14]), both in the phase space and for different parameters [14]. The interplay of chaotic and regular regions affected by quasiperiodic forcing results in the formation of SNAs [4]. The role of chaotic sets in the present case could have been played by the fractal basin boundaries and chaotic attractors of the unforced map. We point out that when chaotic transients are large they delay the formation of SNAs: One may get SNAs if one waits long enough. Since multistability is reduced due to forcing, the observed SNAs are the ones that are born out of the N-band torus with the largest basin of attraction. In the unforced case, this would naturally be the N-period orbit with the largest basin of attraction, and here this is $N = 2$. This may be expected since period-2 orbits have the largest range of existence in the nonlinearity a in the low-dissipation regime, as can be seen in Fig. 5 of Ref. [16]. Moreover, quasiperiodic forcing truncates the sequence of period doubling, leading to chaos [4]. The SNAs reported here are born through the fractalization route, which is well understood [24].

Thus in a weakly dissipative system, forcing creates SNAs out of tori with the largest basin of attraction. It should be noted that long chaotic transients can hinder the detection of SNAs. In addition, the range (in parameter space) for detecting SNAs is reduced in the limit $|1 - \nu| \to 0$ as this is related to the reduced "chaotic area" in the unforced case. Such behavior appears to be generic and can also be seen in other weakly dissipative systems such as the Ikeda map [1,25].

ACKNOWLEDGMENTS

We thank Awadhesh Prasad for comments on the manuscript. S.B. is supported by the CSIR-India through a senior research fellowship (SRF) and RR by the DST through the JC Bose fellowship.

[1] A. P. Kuznetsov, A. V. Savin, and D. V. Savin, Physica A **387**, 1464 (2008).
[2] S. Kraut, U. Feudel, and C. Grebogi, Phys. Rev. E **59**, 5253 (1999).
[3] *Handbook of Chaos Control*, 2nd ed., edited by E. Schöll and H. Schuster (Wiley-VCH, Weinheim, 2008).
[4] U. Feudel, S. Kuznetsov, and A. Pikovsky, *Strange Nonchaotic Attractors* (World Scientific, Singapore, 2006).
[5] V. I. Arnold, *Mathematical Methods of Classical Mechanics (2/e)* (Springer-Verlag, Berlin, 1989).
[6] T. C. Bountis, Physica D **3**, 577 (1981).
[7] S. Kraut and U. Feudel, Phys. Rev. E **66**, 015207 (2002).
[8] B. K. Goswami, Phys. Rev. E **78**, 066208 (2008).
[9] C. S. Rodrigues, C. Grebogi, and A. P. S. de Moura, Phys. Rev. E **82**, 046217 (2010).
[10] C. Murakami, W. Murakami, and K. Hirose, Chaos Solitons Fractals **14**, 1 (2002).
[11] B. V. Chirikov, Phys. Rep. **52**, 263 (1979).
[12] G. Zaslavsky, *The Physics of Chaos in Hamiltonian Systems* (Imperial College Press, London, 2000).
[13] O. Sosnovtseva, U. Feudel, J. Kurths, and A. Pikovsky, Phys. Lett. A **218**, 255 (1996).
[14] U. Feudel and C. Grebogi, Phys. Rev. Lett. **91**, 134102 (2003).
[15] R. V. Mendes, arXiv:chao-dyn/9904004v1.
[16] U. Feudel and C. Grebogi, Chaos **7**, 597 (1997).
[17] L. C. Martins and J. A. C. Gallas, Int. J. Bifurcation Chaos **18**, 1705 (2008).
[18] M. Hénon, Commun. Math. Phys. **50**, 69 (1976).
[19] U. Feudel, C. Grebogi, B. R. Hunt, and J. A. Yorke, Phys. Rev. E **54**, 71 (1996).
[20] J. F. Heagy and S. M. Hammel, Physica D **70**, 140 (1994).
[21] K. Kaneko, *Collapse of Tori and Genesis of Chaos in Dissipative Systems* (World Scientific, Singapore, 1986).
[22] A. Prasad, V. Mehra, and R. Ramaswamy, Phys. Rev. E **57**, 1576 (1998).
[23] J. C. Sprott, Elec. J. Theor. Phys. **3**, 12 (2006).
[24] S. Datta, R. Ramaswamy, and A. Prasad, Phys. Rev. E **70**, 046203 (2004).
[25] K. Ikeda, H. Daido, and O. Akimoto, Phys. Rev. Lett. **45**, 709 (1980).